ELSEVIER

PII: S0144-8617(96)00081-1

*Carbohydrate Polymers* 30 (1996) 101–108

0144-8617/96/$15.00 + .00

# Dynamic mechanical properties of aqueous gellan solutions in the sol–gel transition region

**Kunio Nakamura, Yutaka Tanaka & Masao Sakurai**

*Division of Biological Science, Faculty of Science, Hokkaido University, Sapporo 060, Japan*

Influence of the gelation of aqueous gellan solutions on the dynamic viscoelastic behavior was investigated. Dynamic shear moduli for aqueous gellan solutions (0.60–3.0wt%) were determined over the frequency range from 0.01 to 10Hz and the temperature range from 10 to 60°C by the method of annular pumping between coaxial cylinders. Cole–Cole diagrams in the complex viscosity were constructed, considering temperature and frequency as variables. The complex viscosity was characterized by the circular arc in the viscoelastic gel region and by the skewed circular arc in the sol region. The change in the relaxation from circular arc to skewed circular arc caused by gelation was interpreted in terms of the change in the frequency dependency from the Cole–Cole type to the Williams–Watts type. Copyright © 1996 Elsevier Science Ltd

## INTRODUCTION

Carbohydrate polymers are widespread in nature, and are known to play important roles in all life stages of the organisms. There have been, therefore, many detailed investigations into their aqueous systems over a long period. It is now well recognized that many natural polysaccharides are very important materials in the field of food science and technology and have been used as, for instance, emulsion stabilizers, water absorption agents, gelling and thickening agents etc. (Nishinari & Yano, 1990; Nishinari & Doi, 1993).

Gellan gum, a kind of extracellular microbial polysaccharide, has attracted special interest recently. It was obtained first from the bacterium *Pseudomonas elodea*, under aerobic fermentation conditions, by the Kelco Division of Merck & Co. Inc., USA in 1970. The chemical structure of gellan has been confirmed as a linear anionic heteropolysaccharide consisting of 1,3-β-D-glucose, 1,4-β-D-glucuronic acid, 1,4-β-D-glucose and 1,4-α-L-rhamnose as the repeat unit (Jansson *et al.*, 1983). The native gellan gum contains one glycerate per repeating unit and one acetate approximately every second repeating unit. The $K^+$-form of the gum in which the acyl substituents have been removed is marketed by Kelco as KELCOGEL gellan gum.

Gellan is soluble in water at temperatures above 90°C and on cooling the solution forms a transparent gel at 30–35°C. The more stable rigid gels can be formed by the addition of cations, especially divalent cations such as $Ca^{2+}$ (Crescenzi *et al.*, 1986). The gel formed is known to be heat resistant and its gel strength is less dependent on pH compared to other common polysaccharides gels (Sanderson, 1990). Furthermore, gelation takes place at very low concentrations without syneresis (Meer, 1977). These characteristics are very useful in food applications and, therefore, the polysaccharide has been extensively investigated despite only being commonly available for not much more than a decade. Gellan gum has also been used as a medium in biotechnology and after approval for food use in Japan in 1988, more extensive studies have been performed on its solution properties and gelation phenomena.

As is often the case with biopolymers, however, the results reported from many research groups cannot be compared because of the differences in the sample used. For example, the molecular weight of gellan has been roughly reported to be $100–200\times10^4$ in an earlier study (Glicksman, 1977). However, recent estimations for the soluble tetramethylammonium-type gellan by osmotic pressure and light scattering measurements have revealed much smaller molecular weights: Mn = 5.5 (Ogawa, 1993) and $25\times10^4$ (Milas *et al.*, 1990) and $M_w = 23.8$ (Okamoto *et al.*, 1993) and $43.4\times10^4$ (Dentini *et al.*, 1988). In order to elucidate more clearly the conformation of gellan in solution and the gelation mechanism, it is desirable to investigate the same sample using several techniques. For this purpose, the research group on gellan gum was organized in 1991 by the Research Group on Polymer Gels affiliated to the Society of Polymer Science, Japan.

It has been known that the gellan molecule shows a structural change from a random coil (single strand) at

higher temperatures to an ordered state (double helix) at lower temperatures (Milas *et al.*, 1990). The transition temperature is about 35°C, that is, the gelation temperature as was described above. It can be expected, therefore, that the gelation of gellan relates closely to the conformational change of gellan molecules. As is well-known, the conformational transition of biopolymers is caused by various interactions such as electrostatic, hydrogen-bonding, van der Waals and hydrophobic interactions.

The aqueous gellan solution undergoes the thermally-induced sol-to-gel transition. The solution is a sol at high temperatures. When the solution is cooled, the gelation takes place at a certain temperature depending on the concentration of gellan and added salts. It has been shown that the thermally-induced sol-to-gel transition is related to a coil–helix conformational change for the polymer in solution (Djabourov *et al.*, 1988). The domain structure formed by the nested helices acts as the junction zone for the infinite networks. It is well-known that viscoelasticities in the sol state can be described by a mechanical model for liquids and those in the gel state by a mechanical model for solids. It appears that a time-temperature superposition principle or the reduced variables method (Ferry, 1970) could not be applied to the viscoelastic data of the gellan solutions over the whole temperature range. Accordingly, we attempted to determine the parameters with respect to the viscoelastic strength, relaxation rate, and distribution by using the proper matching function (Tschoegel, 1989) for the dynamic data at each temperature. The objective of this paper is to report the results of dynamic shear moduli of the gellan solutions and to elucidate the relationship between gelation and the conformational change of the gellan molecules.

## EXPERIMENTAL

### Solution preparation of gellan and viscoelastic measurements

Powdered gellan in the deacetylated form was supplied by the Kelco Division of Merck & Co. Inc. It was used without further purification. Viscoelastic measurements were made on five gellan solutions from 0.6 to 3.0% (w/w). The frequency dependence of the storage $G'$ and the loss modulus $G''$ for the solution was measured over the frequency range of 0.01–10Hz at various temperatures. The gellan sample was dissolved in water at 90°C for 20 min to prepare a solution. A solution at first was kept at 90°C and poured into the sample cell, which was heated to the given temperature beforehand. $G'$ and $G''$ were determined at successively lower temperatures in the temperature range of 60–10°C. In the present study, the solutions were maintained at each temperature for 20 min. The apparatus used for viscoelastic measurement has been described elsewhere (Nakamura *et al.*, 1993).

## RESULTS

### Temperature dependence of complex viscosity

*0.60 and 0.81% solutions*

The frequency dependencies of the real part $\eta'$ and the imaginary part of $\eta''$ of the complex viscosity for a 0.81% solution of gellan in water at various temperatures are illustrated in Fig. 1 in a double-logarithmic plot over four decades of frequency. The examination of the frequency dependence of $\eta'$ and $\eta''$ clearly shows that $\eta'$ does not change with frequencies used above 32°C, and in this region the elasticity was so small that we could not determine $\eta''$ values. Actually, the 0.81% solution above 32°C in the measured frequency region behaves as a pure viscous liquid. In the temperature range 32–10°C, a frequency dependence for $\eta'$ and $\eta''$ gradually appears.

In order to classify the domain applicable to the superposition principle, the experimental results were represented in the complex plane. The Cole–Cole plot diagrams are constructed considering temperature and frequency as variables. $\eta'$ and $\eta''$ are divided by a

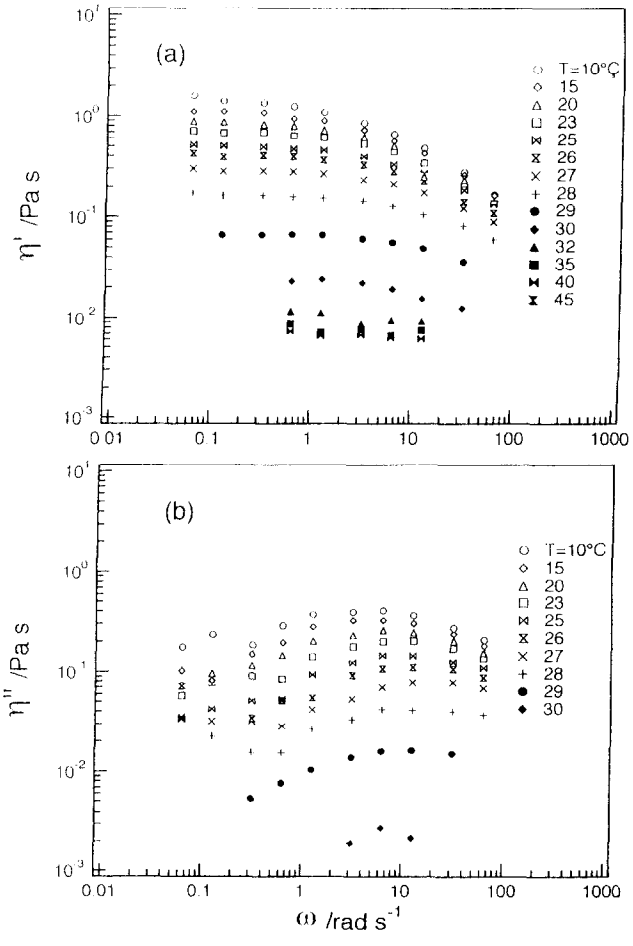


**Fig. 1.** The real part $\eta'$ (a) and imaginary part $\eta''$ (b) of the complex shear viscosity plotted logarithmically against angular frequency for 0.81% gellan solution at various temperatures as indicated.

constant $\eta_p$ so that the data for a solution at different temperatures are superimposed to a most probable normalized matching function. This type of the plot will be termed the reduced Cole–Cole plot.

The reduced Cole–Cole plot of the 0.60% solution at different temperatures is shown in Fig. 2. Figure 2(a) shows the reduced Cole–Cole plot for the 0.6% solution. $\eta'$ and $\eta''$ data in the temperature range 25–10°C form a skewed arc. In Fig. 2(b) master curves of the normalized $\eta'$ and $\eta''$ was shown at the reference temperature $T_s = 25$°C. It is evident that time–temperature superposition rule is valid for this temperature range. The skewed arc obtained from the normalized complex viscosity $\eta^*(\omega)/\eta_p$ was matched to the following Williams–Watts function (Williams & Watts, 1969):

$$\eta N^*(\omega/\omega_0)\eta M_p = \mathrm{L}[\mathrm{G(t)}] \quad (1)$$

where G(t) is relaxation modulus and L[G(t)] indicates the Laplace transform. Here, we assume that G(t) is related to the so-called Kohlrausch function, $\phi$(t) by the following equations:

$$\phi(t) = \exp[-(t/\tau_0)^k](0 < k < 1)$$

$$G(t) = -(d/dt)\phi(t) = [(k/\tau_0)(t/\tau_0)^{-(1-k)}\exp(t/\tau_0)^k] \quad (2)$$

where $\tau_0$ is a characteristic relaxation time and the reciprocal of $\tau_0$ is defined as a characteristic relaxation rate $\omega_0$. The calculation of $\eta^*(\omega/\omega_0)$ having a given value of $k$ in the range 0–1 has been reported by Williams *et al.* (1970).

The relaxation behavior of the 0.6% solution was essentially described by the viscoelastic liquid model, because the Cole–Cole plot of $\eta'$ and $\eta''$ forms an arc at low frequencies (right-hand side of arc). Therefore, $\eta_p$ indicates the steady-state viscosity $\eta_0$. The reduced Cole–Cole plot and master curves of the normalized $\eta'$ and $\eta''$ for the 0.81% solution are shown in Fig. 3(a) and (b), respectively. The rheological features for the 0.81% solution are quite similar to those for the 0.6% solution except that the transition region shifts to higher temperature with increasing gellan concentration.

$\eta_0$ and $\omega_0$ for the 0.6 and 0.81% solutions determined by constructing the reduced Cole–Cole plot are shown in Fig. 4. The viscoelastic feature for the 0.6% solution are separated into three regions in the whole temperature range; (1) $T > 29$°C, the pure viscous region; (2) $29 > T > 25$°C, the transition region characterized by the steep increase in $\eta_0$ and $\omega_0$ with decreasing temperature; (3) $25 > T > 10$°C, the region in which time–temperature superposition is applicable and $\omega_0$ decreases with decreasing temperature. We denote the transition temperature, 29°C, from (1) to (2) as $T_g^+$, and that, 25°C from (2) to (3) as $T_g^-$. $T_g^+$ and $T_g^-$ for the 0.81% solution are 32 and 27°C, respectively.

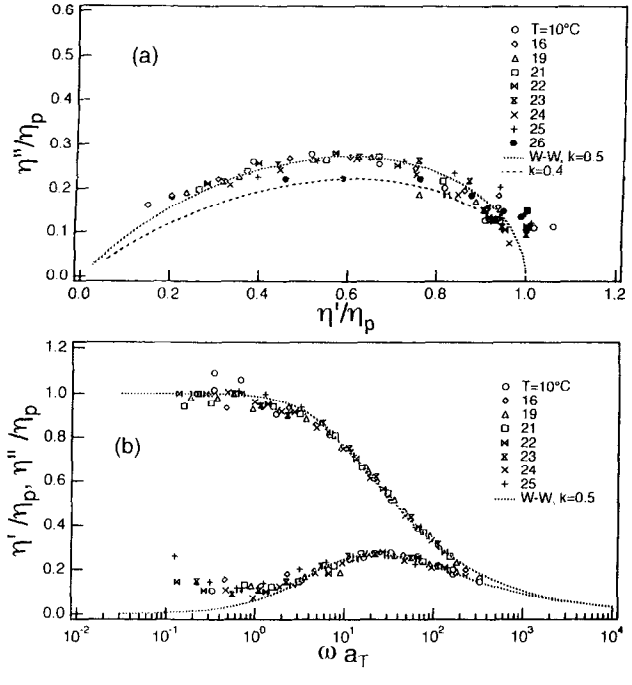


**Fig. 2.** Reduced Cole–Cole plots (a) and master curve (b) of 0.60% aqueous solution at various temperatures as indicated. (a) $\eta_p$ values at 26, 25, 24, 23, 22, 21, 19, 16, and 10°C are 0.071, 0.15, 0.23, 0.27, 0.33, 0.37, 0.44, 0.56, and 0.75Pa.s, respectively. The lines are Williams–Watts function characterized by $k = 0.5$ and 0.4 as indicated. (b) The reference temperature was taken as $T = 25$°C.

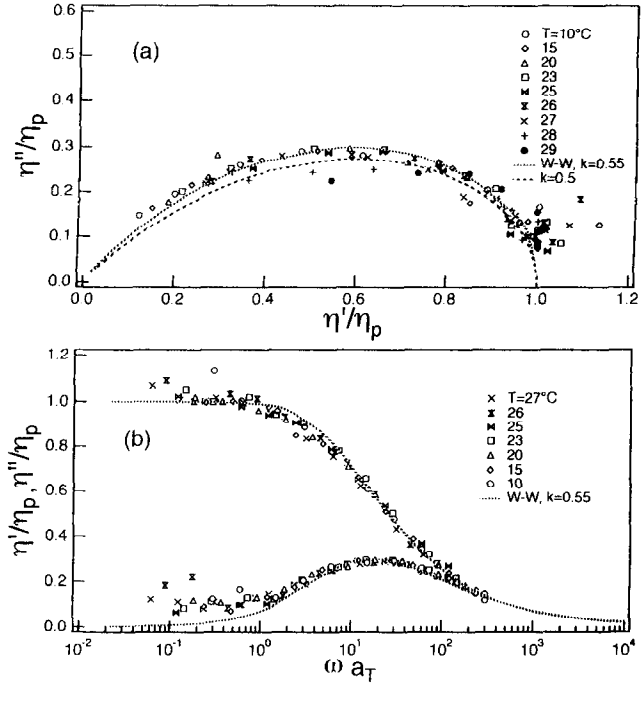


**Fig. 3.** Reduced Cole–Cole plots (a) and master curve (b) of 0.81% aqueous solution at various temperatures as indicated. (a) $\eta_p$ values at 29, 28, 27, 26, 25, 23, 20, 15 and 10°C are 0.066, 0.16, 0.28, 0.39, 0.50, 0.67, 0.86, 1.10, and 1.39Pa.s, respectively. The lines are Williams–Watts function characterized by $k = 0.55$ and 0.5. (b) The reference temperature was taken as $T = 27$°C.

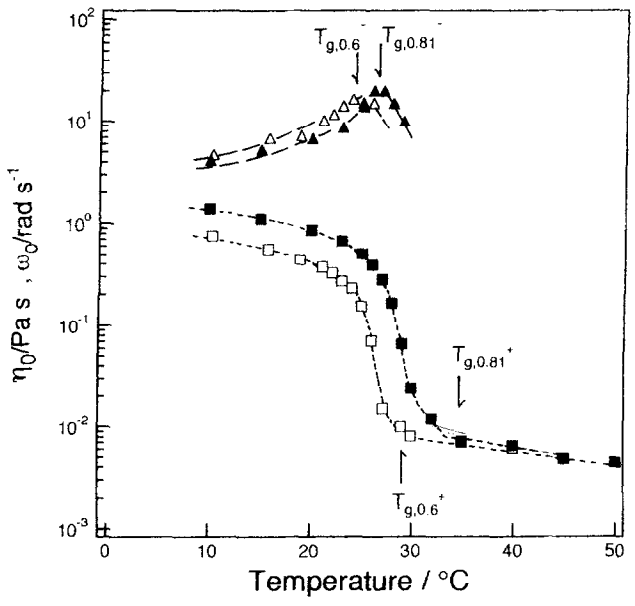


**Fig. 4.** The temperature dependence of steady-state viscosity $\eta_0$ and characteristic relaxation rate $\omega_0$ for 0.60 (open symbol) and 0.81% (closed symbol) solutions.

*1.0, 1.5, and 3.0% solutions*

$\eta'(\omega)$ and $\eta''(\omega)$ for a 1.0% solution at various temperatures are plotted double-logarithmically against frequency in Fig. 5. The frequency dependence of $\eta'$ for a 1.0% solution at lower frequencies and lower temperatures is quite different from that for the 0.6 or 0.81% solution. $\eta''$ for the 0.81 solution (see Fig. 1) decreases steeply with decreasing frequency. On the other hand, $\eta''$ for the 1.0% solution increases with decreasing frequency, thus the elastic contribution is obvious. Figure 6 shows the reduced Cole–Cole plot for the 1.0% solution. $\eta'$ and $\eta''$ at 32.5, 31, and 30°C form a skewed arc (Fig. 6(a)). Data in this temperature range are fitted to the Williams–Watts function.

Data in the temperature range 29–10°C forms a circular arc (Fig. 6(b)) at higher frequencies (left-hand side of the arc). The deviation from the arc at lower frequencies reflects the elastic effect. It was found that the viscosities in this temperature range were fitted to the following Cole–Cole function (Cole & Cole, 1941) which includes an elastic component of modulus $G_e$:

$$\eta^*(\omega) = G_e/\omega + \eta_p/[1 + (i\omega/\omega_0)^{\beta}](0 < \beta < 1) \quad (3)$$

where $\omega_0$ is a characteristic relaxation rate and $\omega$ an angular frequency. $G_e$ is an equilibrium modulus or gel modulus. The exponent $\beta$ in Equation 3 may relate to the distribution of relaxation times. Equation 3 is reduced to the Zener model when $\beta = 1$.

By assuming that the deviation of $\eta''/\eta_p$ at lower frequencies comes from $G_e$ in Equation 3, we determined $G_e$ from the $[\eta''-(G_e/\omega)]/\eta_p$ vs $\eta'/\eta_p$ plot (Fig. 6(c)). Thus, the 1.0% solution undergoes obviously the transition from a viscoelastic liquid to a viscoelastic solid with decreasing temperature. The former was expressed by a non-symmetrical mechanical relaxation behavior, the latter by a symmetrical one.

It should be noticed that the data of $\eta'$ and $\eta''$ for the 1.0% solution at 32.5, 31, and 30°C cannot be combined by the method of reduced variables. More especially, the steady-state viscosity $\eta_0$ and $\omega_0$ at 29°C cannot be determined because $\eta''$ at low frequencies is parallel to the abscissa (see Fig. 6(a)). In this case, the frequency dependence of the dynamic viscosity at 29°C in the low frequency region is characterized by $\eta''$ remaining constant and an appreciable increase in $\eta'$ (Fig. 5) with decreasing the frequency. On the other hand, data at higher frequencies were fitted to the Williams–Watts function. Nakamura *et al.* (1992) have shown the same type behavior in a study of thermoreversible gelation for aqueous poly (methacrylic acid).

Hess *et al.* (1988) and Vilgis & Winter, (1988) have shown in a series of papers that dynamic mechanical measurements provide a technique for detecting gelation precisely. For the critical gel state between sol and

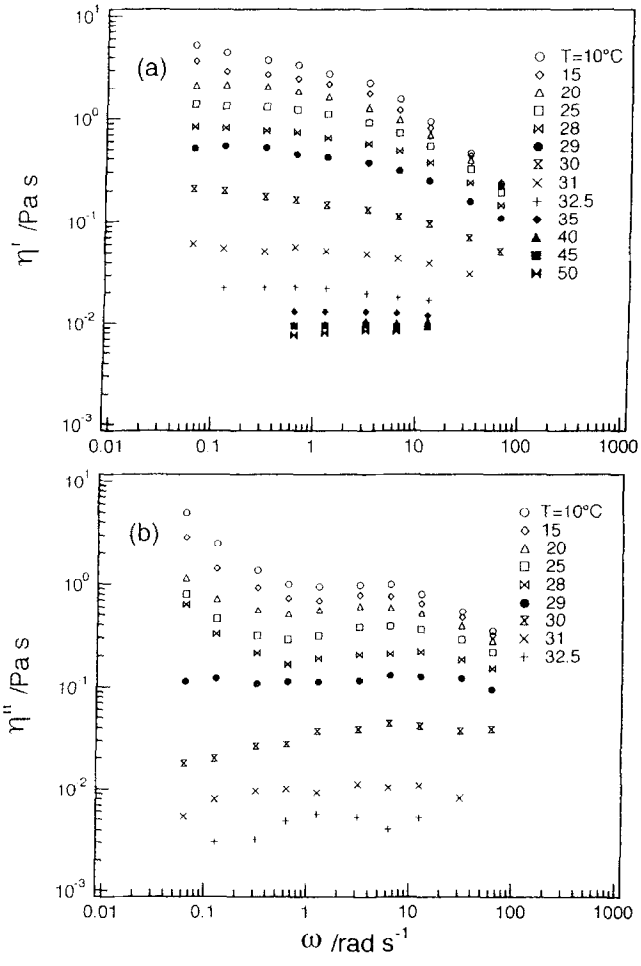


**Fig. 5.** The real part $\eta'$ (a) and imaginary part $\eta''$ (b) of the complex shear viscosity plotted logarithmically against angular frequency for 1.0% gellan solution at various temperatures.

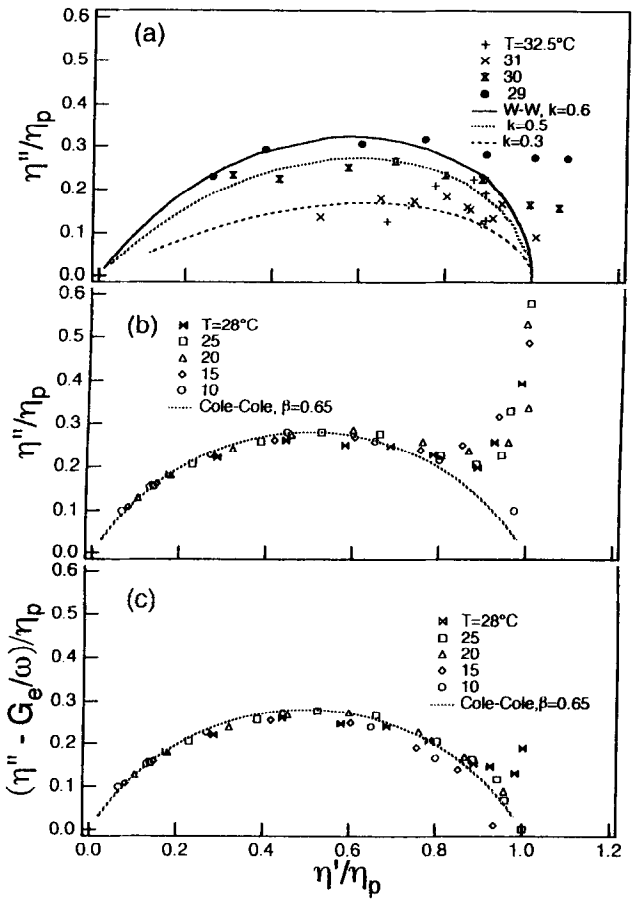


**Fig. 6.** Reduced Cole–Cole plots of 1.0% aqueous solution at various temperatures as indicated. (a) $\eta_p$ values at 32.5, 31, 30, and 29°C are 0.022, 0.070, 0.18, and 0.45Pa.s, respectively. The lines are Williams–Watts function characterized by $k$ as indicated. (b) $\eta_p$ values at 28, 25, 20, 15, and 10°C are 0.83, 1.38, 2.14, 2.90, and 3.46Pa.s, respectively. The dotted line is Cole–Cole function characterized by $\beta = 0.65$. (c) $G_e$ values at 28, 25, 20, 15, and 10°C are 0.003, 0.006, 0.01, 0.021, and 0.042Pa, respectively. The dotted line is the Cole–Cole function characterized by $\beta = 0.65$.

gel, the complex viscosity could be expressed by the following power law (Tschoegel, 1989) over a wide frequency range:

$$\eta^*(\omega) = (1/i\omega)G^*(i\omega/\omega_0)^n (0 < n < 1) \quad (4)$$

$$\tan(n\pi/2) = \eta'/\eta''.$$

The simple power law relaxation with $n = 0.5$ over a wide frequency range has already been shown in a study of dynamic behavior for chemical gelation and vulcanization of polymers. However, we did not observe the simple power law relaxation. This discrepancy in the critical gel behavior needs to be investigated further. We tentatively determined the gelation temperature $T_g$ at which this peculiar relaxation behavior was observed. $G_e$, $\eta_0$, and $\omega_0$ are shown in Fig. 7. The viscoelastic feature accompanying gelation for the 1.0% solution are separated into four classes over the whole temperature range: (1) $T > 35$°C, the pure viscous region; (2) $35 > T > 30$°C, the transition region characterized by the steep increase in $\eta_0$ and $\omega_0$ with decreasing temperature; (3) $28 > T > 10$°C, the transition region characterized by the steep increase in $G_e$ and the decrease in $\omega_0$, with decreasing temperature; (4) $T = 29$°C, at which the relaxation behavior was not fitted over the measured frequency range to the matching function presently considered. The relaxation behavior for a 1.5% solution is similar to that for the 1.0% solution, but the transition region from sol-to-gel shifts to higher temperatures with the increase in concentration. The parameters obtained by analyzing data using the same treatment as for the 1.0% solution are also shown in Fig. 7. As can be seen in Fig. 7, $T_g$ and $T_g^+$ are 32.5 and 40°C, respectively, and the elastic contribution to the dynamic viscosity is larger than that for the 1.0% solution.

$\eta'(\omega)$ and $\eta''(\omega)$ for a 3.0% solution at several temperatures are plotted double-logarithmically against frequency in Fig. 8, together with the adopted matching function. $G_e$, $\eta_0$, and $\omega_0$ values are shown in Fig. 7. The data in the temperature range from 47 to 42°C were fitted to the Williams–Watts function with $k = 0.3$–$0.5$, and $T_g$ is 41°C. The dynamic viscosity data at lower temperatures ($T = 40$–$32$°C) were described by the Cole–Cole function with $\beta = 0.65$, the same as the 1.0 and 1.5% solutions. However, the pure elastic term $G_e/\omega$ in $\eta''$ at 25 and 30°C becomes so large that the maximum in $\eta''$ is not observed, and $\beta$ increases appreciably.

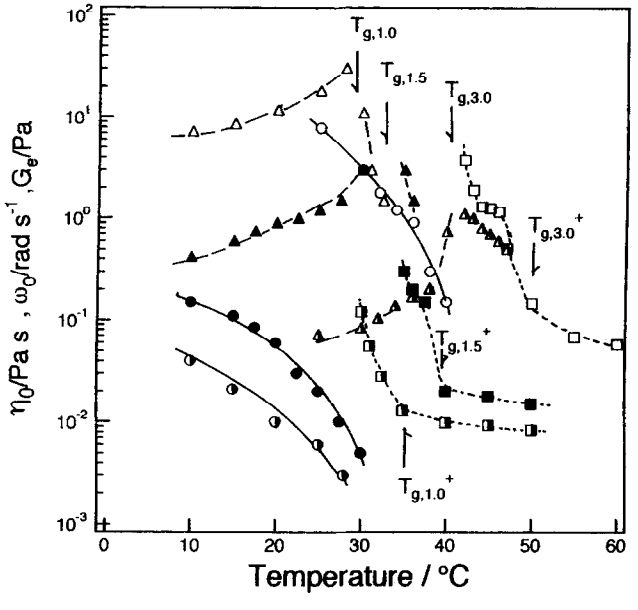


**Fig. 7.** The temperature dependence of the steady-state viscosity $\eta_0$, gel modulus $G_e$ and characteristic relaxation rate $\omega_0$ for 1.0, 1.5 and 3.0% solutions. Circles denote $G_e$, triangles $\omega_0$, and squares $\eta_0$. Open symbols denote 3.0%, filled symbols 1.5%, and half-filled symbols 1.0%.

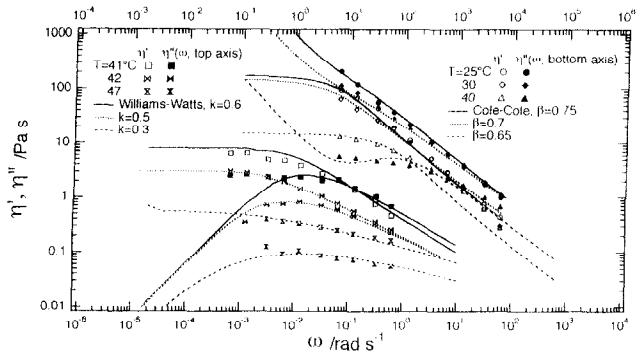


**Fig. 8.** The angular frequency dependence of the complex viscosity for 3.0% aqueous gellan solution at 47, 42, 41, 40, 30 and 25°C. The lines are matching functions used to fit to data as indicated.

## DISCUSSION

### Temperature dependence of power law index, $G_e$, $\eta_0$, and $\omega_0$

In order to classify the matching function, G′ and G″ calculated from the dynamic viscosity data shown in Fig. 8 for the 3.0% solution are plotted double-logarithmically against frequency in Fig. 9. In the previous section, we analyzed the viscoelastic properties in terms of the dynamic viscosity to clarify this feature of the viscoelasticity at lower frequencies where the solution in the sol and gel state behave differently. It is more convenient to use the dynamic moduli G′ and G″ to characterize viscoelasticity at higher frequencies. The dynamic moduli for the matching function of Cole–Cole and those for Williams–Watts obey power laws as $\omega/\omega_0 > > 1$. However, the most important difference between the Cole–Cole and Williams–Watts function at higher frequencies is the tendency for power law behavior for the Williams–Watts function to begin faster than for the Cole–Cole function. If we consider the viscoelastic behavior in relation to the matching function, the transition from aggregation state, in other words, pre-gel state to gel state, can be anticipated. The exponent for the modulus of the Cole–Cole function is $1-\beta$, and that of Williams–Watts function $1-k$. $1-\beta$ and $1-k$ for aqueous Gellan solutions are plotted against temperature in Fig. 10. The exponent for the pure viscous liquid is 1 (Equation 4 with $n=1$). This parameter clearly characterizes the solution state in sol and gel. When the exponent is larger than 0.4 the solution behaves as a sol. We could not observe in the present study the behavior of the pure elastic gel for which the exponent is zero (Equation 4 with $n=0$).

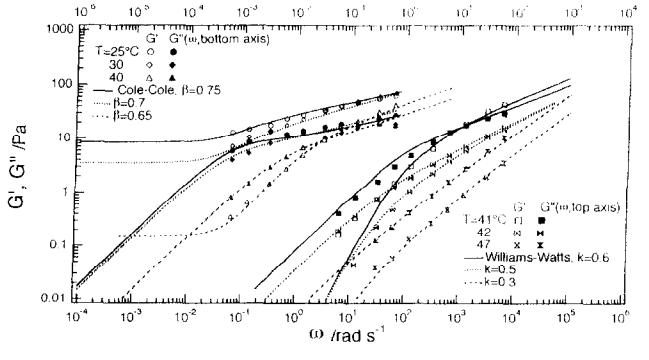


**Fig. 9.** The angular frequency dependence of the complex modulus for 3.0% aqueous gellan solution at 47, 42, 41, 40, 30, and 25°C. All data and lines were those calculated by using the relation $G^*(\omega) = i\omega\eta^*(\omega)$, as shown in Fig. 8.

As was seen in Figs 4 and 7, with decreasing temperature, the viscosity $\eta_0$ for the 0.6 and 0.81% solutions increases at first slightly, followed by an abrupt increase in $\eta_0(T_g^+)$, and then increases weakly, $T_g$ . The increase in $\eta_0$ below $T_g^-$ in the gelation process may be a similar phenomenon to vitrification, because a time–temperature superposition rule is applicable and the characteristic relaxation rate $\omega_0$ decreases with decreasing temperature. $T_g^+$ and $T_g^-$ for the 0.6% solution are 29 and 25°C, those for the 0.81% solution are 32 and 27°C. These results suggest that gelation occurs over a small temperature step, although these solutions do not form gels ($G_e = 0$). In this transition region, $\omega_0$ increases with decreasing temperature in parallel with $\eta_0$. $\omega_0$ may be scaled as $\omega_0 = G/\eta_0$ (refer to Equation 3 with $\beta = 1$). We note that G is not the modulus at low frequencies but at high frequencies ($\omega/\omega_0 > > 1$). This phenomenon may be explained by assuming that the temperature dependence of G is much bigger than that of $\eta_0$.

The 1.0, 1.5, and 3.0% solutions form gels (Fig. 7). $T_g$ and $T_g^+$ for the 1.0% solution are 29 and 35°C. Below $T_g$,

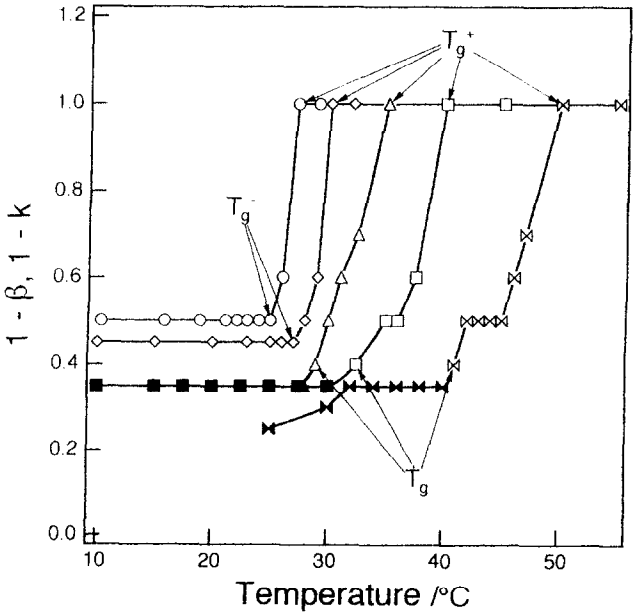


**Fig. 10.** $1-\beta$ and $1-k$ of aqueous gellan solutions of various concentrations plotted against temperature. (○); 0.6%, (◇); 0.81, (△); 1.0%, (□); 1.5, (▷◁); 3.0. Open symbols denote $1-k$, filled symbols $1-\beta$.

a time–temperature superposition rule is applicable to the viscoelastic part of the dynamic viscosity and the characteristic relaxation rate $\omega_0$ decreases with decreasing temperature. Therefore, gelation essentially occurs in the temperature range $T_g^+ - T_g$. By decreasing temperature further, the increase in the number of junction zones in the gel network may follow. $T_g$ and $T_g^+$ for the 1.5 and 3.0% solution are 32.5 and 40, and 41 and 50°C, respectively. The larger the gellan concentration, the more the difference between $T_g^+$ and $T_g$. It is evident that there is an aggregation state (Equation 1 with $k=0.5$) in the temperature range 45–42°C (Fig. 10). This two-step gelation becomes more obscure with decreasing concentration. It was considered that in order to form infinite networks, the gellan molecules may recombine in the process from the aggregation state to the gel states. The most promising explanation seems to be that the broader transition at higher concentrations comes from the increase in the solution viscosity.

Taking the gelation temperature as $T_g$, $G_e$ and $\eta_0$ were plotted double-logarithmically against the reduced temperature in Fig. 11. The exponent of $G_e$ is 2.0 in $(T/T_g)-1$, range of 0.01–0.05, and that of $\eta_0$ is 1.0 in $1-(T/T_g)$, range of 0.003–0.02. The exponent of the gel modulus and viscosity with respect to the reduced helix content for aqueous gelatin is 1.82 and 1.48 (Djabourov *et al.*, 1988). Details of the exponent will be reported at a later date.

**Phase diagram characterized by the matching functions**

Finally, we summarized the aqueous gellan solution in various states by phase diagram which was determined by the difference in the rheological behavior (Fig. 12).

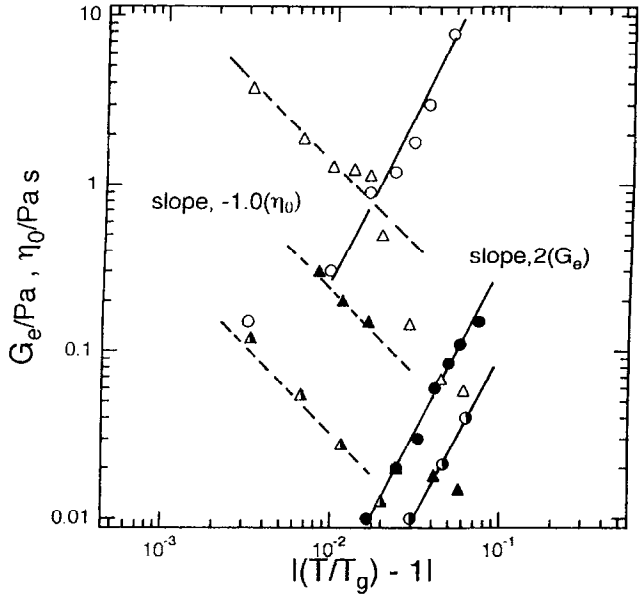


**Fig. 11.** The gel modulus and viscosity of aqueous gellan solutions of various concentrations plotted logarithmically against reduced temperatures. $G_e$;(○) 3.0, (●) 1.5, (◑) 1.0%. $\eta_0$; (△) 3.0, (▲) 1.5, (◭) 1.0%.

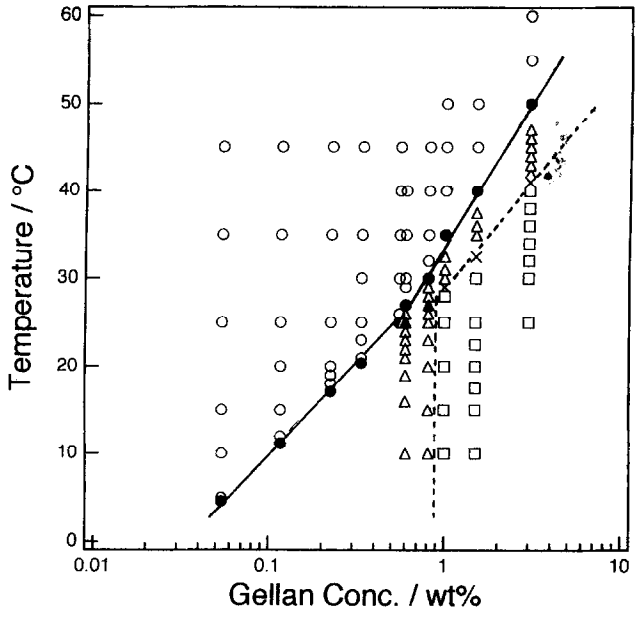


**Fig. 12.** Phase diagram of aqueous gellan solutions. Open circles denote the viscous region and filled circles the onset temperatures of the increase in viscosity ($T_g^-$). Open triangles denote the Williams–Watts type relaxation and filled triangles $T_g^-$. Open squares denote gel region of Cole–Cole type relaxation. Cross were $T_g^-$. Data below gellan conc. 0.55% were taken from ref. (Sakurai *et al.*, 1995).

This shows the previous result in the dilute regime from viscometry (Sakurai *et al.*, in press).

The viscoelastic behavior of the aqueous gellan solution are classified into three regions in the temperature and concentration range: (1) the pure viscous region (circles) where gellan in solution is in the coil state; (2) the viscoelastic liquid region (triangles) characterized by the Williams–Watts function; (3) the viscoelastic solid region in which the solution forms gel (squares). The dotted line shows the gelation curve and the solid line the point where a steep increase in the steady shear viscosity starts to be observed. In region (2) the solution probably does not form a gel, although the aggregation of gellan chains occurs appreciably. This aggregation temperature steadily decreases with decreasing gellan concentration. On the other hand, the gelation temperature at first decreases with decreasing concentration and then does not depend on the gellan concentration, that is, gelation does not occur below a certain concentration between 0.81 and 1.0%. This result indicates that a minimum gelling concentration exists. This concentration for the present gellan is between 0.81 and 1.0%. $C_{mg}$ of the gellan used (potassium-type) in the previous study is 0.3% (Nakamura *et al.*, 1993). So the gelation ability of gellan (sodium-type) used in the present study is quite poor.

It is of interest to compare the rheological data with the ultrasonic velocities and CD data on the same gellan previously studied (Tanaka *et al.*, in press). We have suggested that the aqueous gellan solution undergoes

the conformational change at the transition temperature $T_c$ characterized by CD spectrum (Dentini *et al.*, 1988) and the ultrasonic velocities (Tanaka *et al.*, 1993). $T_c$ for a 0.81% solution is 27°C and that for a 1.0% solution 29°C (Tanaka *et al.*, 1996). These values are in agreement with $T_g^-$ for the 0.81% solution and $T_g$ for the 1.0% solution.

The crosslink forming process with decreasing temperature can be considered to be a series reaction of the type, A → B → C. In this case, A represents cross linking sites which are unreactive because they are in the coil form. B represents potential crosslink sites which are reactive but have not yet formed cross links. C represents permanent crosslinks.

There are two fundamental reactions in this process. The first reaction is the conversion of unreactive sites into potential sites. This reaction involves the conformational change of gellan molecules to form double helices (Yuguchi *et al.*, 1993; Robinson *et al.*, 1991). The second is the aggregation reaction of helices to form junction zones. The underlying idea is that the coil must completely be changed to helices before aggregation can start. However, it has never been established that the two reactions proceed separately. The gelation temperature is in accordance with $T_c$ near the minimum concentration of gelling. It was considered that both steps may actually start simultaneously and/or the former reaction is predominant and subsequent reaction of the aggregation occurs simultaneously.

## ACKNOWLEDGEMENTS

We wish to thank Dr G. Sanderson, Kelco Division of Merck & Co., and Professor K. Nishinari, Osaka City University, for supplying the gellan sample. We also wish to thank the Tajima Roofing Co. Ltd for their financial support.

## REFERENCES

Cole, K.S. & Cole, R.H. (1941). Dispersion and absorption in dielectrics I: alternating current characteristics. *J. Phys. Chem.*, **9**, 341–352.

Crescenzi, V., Dentini, M., Coviello, T. & Rizzo, R. (1986). Comparative analysis of the behavior of gellan gum (S-60) and welan gum (S-130) in dilute aqueous solution. *Carbohydr. Res.*, **149**, 425–432.

Crescenzi, V., Dentini, M. & Dea, I.C.M. (1987). The influence of side-chains on the dilute-solution properties of three structurally related bacterial anionic polysaccharides. *Carbohydr. Res.*, **160**, 283–302.

Dentini, M., Coviello, T., Burchard, W. & Crescenzi, V. (1988). Solutions properties of exocellular microbial polysaccharides. *Macromolecules*, **21**, 3312–3320.

Djabourov, M., Leblond, J. & Papan, P. (1988). Gelation of aqueous gelatin solutions. II. Rheology of the sol–gel transition. *J. Phys.*, **49**, 333–365.

Ferry, J.D. (1970). *Viscoelastic Properties of Polymers*, 2nd ed., John Wiley, New York, pp. 292–295.

Glicksman, M. (1977) *Food Colloids*. Graham, H.D. (ed.). Avi. Publ. Co., Westport, pp. 270–295.

Hess, W., Vilgis, T.A. & Winter, H.H. (1988). Dynamical critical behavior during chemical gelation and vulcanization. *Macromolecules*, **21**, 2536–2542.

Jansson, P., Lindberg, B. & Sandford, P.A. (1983). Structural studies of gellan gum, an extracellular polysaccharide elaborated by *Pseudomonas elodea*. *Carbohydr. Res.*, **124**, 135–139.

Meer, W.A. (1977). *Food Colloids*. ed. H.D. Graham, Avi Publ. Co., Westport, pp. 531–535.

Milas, M., Shi, X. & Rinaudo, M. (1990). On the physicochemical properties of gellan gum. *Biopolymers*, **30**, 451–464.

Nakamura, K., Itoh, T., Sakurai, M. & Nakagawa, T. (1992). The viscoelastic properties of aqueous poly (methacrylic acid) solutions and their relations to thermoreversible gelation. *Polymer J.*, **24**, 1419–1427.

Nakamura, K., Harada, K. & Tanaka, Y. (1993). Viscoelastic properties of aqueous gellan solutions; the effects of concentration on gelation. *Food Hydrocoll.*, **7**, 435–447.

Nishinari, K. & Yano, T. (eds) (1990). *Science of Food Hydrocolloids*. Asakura, Tokyo (in Japanese).

Nishinari, K. & Doi, E. (eds) (1993) *Food Hydrocolloids — Structures, Properties and Functions*. Plenum Press, New York.

Ogawa, E. (1993). Osmotic pressure measurements for gellan gum aqueous solution. *Food Hydrocoll.*, **7**, 397–405.

Okamoto, T., Kubota, K. & Kuwahara, N. (1993). Light scattering study of gellan gum. *Food Hydrocoll.*, **7**, 363–371.

Robinson, G., Manning, C.E. & Morris, E.R. (1991). Conformational and physical properties of the bacterial polysaccharides gellan, welan, and rhamsan. In ed. E. Dickinson, *Food Polymers, Gels, and Colloids*. Royal Society Chemistry, UK, pp. 22–32.

Sakurai, M., Tanaka, Y. & Nakamura, K. (1995). Viscosities, densities and sound velocities for dilute aqueous gellan solutions. *Food Hydrocolloids*, **9**, 189–194.

Sanderson, G.R. (1990). *Food Gels*, Harris, P. (ed.). Elsevier Applied Science, London and New York, pp. 201–232.

Tanaka, Y., Sakurai, M. & Nakamura, K. (1996). Ultrasonic velocity and circular dichroism in aqueous gellan solution. *Food Hydrocolloids*, **10**, 133–136.

Tanaka, Y., Sakurai, M. & Nakamura, K. (1993). Ultrasonic velocities in aqueous gellan solutions. *Food Hydrocoll.*, **7**, 407–415.

Tschoegel, W. (1989) *The Phenomenological Theory of Linear Viscoelastic Behavior*. Springer, pp. 314–364.

Vilgis, T.A. & Winter, H.H. (1988). Mechanical selfsimilarity of polymers during chemical gelation. *Colloid & Polym. Sci.*, **266**, 494–500.

Williams, G. & Watts, D.C. (1969). Non-symmetrical dielectric relaxation behavior arising from a simple empirical decay function. *Trans. Faraday Soc.*, **65**, 80–85.

Williams, G., Watts, D.C., Dev, S.B. & North, A.M. (1970). Further considerations of non symmetrical dielectric relation behaviour arising from a simple empirical decay function. *Trans. Faraday Soc.*, **66**, 1323–1335.

Yuguchi, Y., Miura, M., Kitamura, S., Urakawa, H. & Kajiwara, K. (1993). Structural characteristics of gellan in aqueous solution. *Food Hydrocoll.*, **7**, 373–385.